PERFORMANCE OF MAGNESIUM CATHODE IN THE S-BAND RF GUN

T. Srinivasan-Rao, I. Ben-Zvi, J. Smedley, X. J. Wang, M. Woodle
Brookhaven National Laboratory, Upton, NY 11973, and
D. T. Palmer, R. H. Miller, SLAC, Stanford University, Stanford, CA, 94305

Abstract

In this paper, we present the preliminary results of the performance of magnesium cathode in a high frequency RF gun. The quantum efficiency of Mg showed a dramatic improvement upon laser cleaning, increasing from 10^{-5} to $4x10^{-4}$ after two hours of cleaning, and to $2x10^{-3}$ after systematic cleaning. The cleaning procedure for this increase is described in detail. Charge measured as a function of the laser injection phase relative to the RF phase indicates that the temporal variation of the field on the cathode both due to the RF and the shielding effect of the emitted electrons play a critical role in the emission and extraction of electrons. A model that includes this variation is numerically fitted to the measured charge and the results are presented. The unexpected outcome of the fit was the low field enhancement factor (0.1) predicted by the model for the photoemission. The physical origin of this is still under investigation.

1 INTRODUCTION

In the past decade, there has been considerable research[1] in identifying a photocathode material that would be both rugged and efficient at the same time. Progress in cesiated materials has resulted [2,3] in quantum efficiencies of a few percent and life times of a few weeks. Metal photocathodes with 0.5% quantum efficiency and infinite life times have been identified[4]. For the first time, such a high quantum efficiency metal has been processed and studied systematically in a RF gun under high fields, and the results are presented in this paper.

2 EXPERIMENTAL ARRANGEMENT

The RF gun used in these experiments is the injector[5] of the Brookhaven Accelerator Test facility (ATF). It is a 1.6 cell, S-band, copper gun with a removable back plate, the center of which acts as the photocathode. The cathode can be illuminated by the ATF photocathode laser system delivering up to 100 μJ of laser energy at 4.66 eV photon energy on the cathode at 72° incident angle. The spatial ellipticity and temporal tilt caused by this oblique incidence were compensated by a pair of prisms and gratings. The spot size of the laser beam on the cathode can be changed by changing the telescoping lenses and imaging apertures in the beam. The laser energy irradiating the gun was measured simultaneously by a calibrated pick-off for laser energies > 10 μJ. For lower energies, an energy meter was inserted in the main beam and the laser energy was measured directly.

A 2-cm diameter, 99.8 % pure, magnesium disc was press fitted in to an indent in the center of the copper back plate of the gun and secured with a bolt in the back. The surface was then machined carefully to be in level with the Cu plate. The center of the plate was then polished with 600 grit soft polishing paper, followed by diamond polishing compound (Beuhler Metadi) of 9, 6, and 1 μm grain size. The plate was then rinsed with hexane and cleaned in an ultrasonic hexane bath for 20 minutes. It was then immediately transported to a vacuum oven where it was backed for 48 hours at 150°C. The plate was then subjected to vacuum-bake-pressurize cycle to ensure good electrical contact at the Cu-Mg interfaces. The back plate was then mounted on to the gun and the system was baked for a week at 200°C before applying the RF. Both the photocurrent and the dark current from the cathode were measured by the Faraday cup immediately after the gun.

3 MEASUREMENTS AND DISCUSSION

3.1 Cleaning Procedure

After conditioning the gun, the quantum efficiency was measured by measuring the emitted charge and the laser energy simultaneously. The cathode was then cleaned with 160 $\mu J/mm^2$ energy without the RF. The QE was measured at different locations on the cathode after irradiation and was found to vary from $9x10^{-5}$ to $6.6x10^{-4}$. The cathode was then slowly scanned with the laser, maintaining a RF field of 67 MV/m on the cathode. At each scan site, the laser energy was adjusted till there was explosive emission from the cathode for at least 3 consecutive shots. After this scan, the QE increased to $2x10^{-3}$ and the variation in QE decreased dramatically to a factor of two. Fig. 1 is a photograph of the magnesium surface when it was removed from the gun. It can be seen from the picture that the surface has been modified during cleaning, but the depth of damage is < 12 μm as measured with a depth gauge. This cathode was in use for more than 3 months, and no irreversible decay in the QE was measured. Breakdowns and arcing in the RF gun tend to reduce the QE. However, the high QE could be restored by repeating the slow scan cleaning procedure. Measurement of charge as a function of the laser energy indicates that for charges <1nC, the collected charge

0-7803-4376-X/98/$10.00

varies linearly with the laser energy for both cases, implying a one photon process for the photoemission.

Fig. 1: Mg cathode surface after being irradiated by the laser, under high magnification.

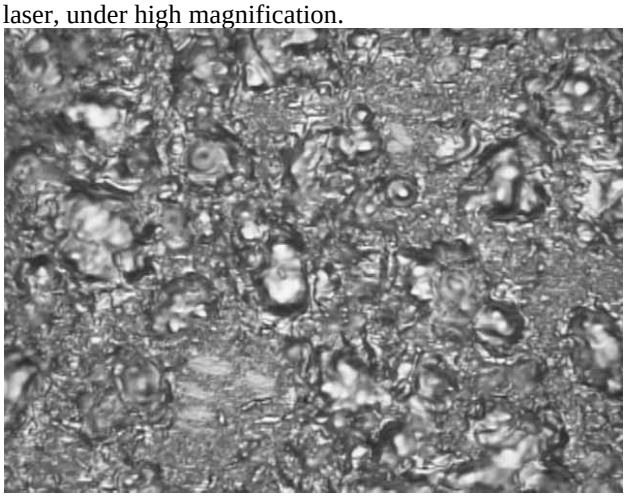

3.2 Dependence of measured charge on the injection phase of the laser

The instantaneous photoelectric current density can be expressed [6] as:

$$\frac{d\sigma}{dt} = AI(t)\left(h\upsilon - \phi + \alpha\sqrt{\beta E(t)}\right)^2 \quad [1]$$

Here I(t) is the intensity distribution of the laser, βE(t) is the surface field at the cathode for a field enhancement of β. A is a material dependent constant, hυ−ϕ is the difference between the photon energy and the work function and $\alpha=3.786\times10^{-5}$ in MKS units. Eq. 1 is integrated over the laser distribution to obtain the total charge density of a bunch injected at a given phase. The field dependent term in Eq. 1 represents the Schottky reduction of the work function [7]. For sufficiently low charge,

$$E(t) = E_0 \sin(\theta + \Delta\theta(t)),$$

the RF field at the cathode, where θ is the injection phase of the laser with respect to the RF, and Δθ is the variation of the RF phase during the laser pulse duration. For higher charges, the surface field should also include the space charge of the preceding electrons,

$$E(t) = E_0 \sin(\theta + \Delta\theta(t)) - \frac{1}{\varepsilon_0}\int_{-\tau}^{t} \frac{d\sigma}{dt'} dt'.$$

τ is the start time of the laser, and ε_0 is the dielectric constant of vacuum

Experimentally, for a constant laser energy and RF field, the injection phase of the laser was varied and the charge at the Faraday cup was measured at each of the phase. The measurements were repeated for different laser energies and RF fields. Each of these data sets was numerically fitted to Eq. 1. Since only the relative phase between the laser and the RF is known, the zero offset for the RF phase was an initial input parameter. The temporal profile of the laser was also an initial input parameter. $A^{1/2}(h\nu-\phi)$ and $(A\beta)^{1/2}$ were used as fitting parameters. It is useful to note that the data can be broken into sections, each section depending primarily on one of the above parameters. The fit at low injection phases depends strongly on the zero offset. The slope in this region is determined by the laser width. The phase at which the Schottky effect becomes significant is determined by the parameter $A^{1/2}(h\nu-\phi)$. Beyond this phase, the slope depends only on $(A\beta)^{1/2}$. The cut off at the high injection phase is due to the electron transport in the gun and is determined by the acceptance energy of the gun and the Faraday cup. The slope of the falling edge is again an indication of the laser width. A Lorentzian temporal profile with a FWHM of 14 ps was used as the laser profile for the low charge data. For high charge, a charge dependent asymmetry was added to the trailing edge of the pulse to account for the change in electron bunch length due to space charge effects. The energy cut off for the low charge data was a γ of 4.5, while for the high charge, higher cut off energies were assumed. Table 1 lists the best fitting parameters for 7 different data sets. Two data sets, one with low charge at 120 MV/m and a laser energy of 1.98 μJ, and another with high charge at 120 MV/m and a laser energy of 10.8 μJ along with their best fits are shown in Fig. 2a and 2b respectively.

Table 1: Best Fitting Results (ϕ=3.66 eV has been assumed) SL: symmetric Lorentzian, ASL: asymmetric Lorentzian, Half Width at Half Maximum of leading edge =7 ps.

E_0 MV/m	Laser Energy μJ	Laser Profile	Zero field QE (10^{-5})	β
120	1.98	SL	6.0	.05
116	1.98	SL	6.1	.09
112	1.98	SL	6.5	.09
105	1.98	SL	6.5	.1
120	3.24	SL	5.6	.11
120	8.14	ASL	6.6	.11
120	10.8	ASL	6.1	.1

As can be seen both from the Table and the Figures, the simple model predicts the emission and transport of electrons fairly accurately. The best fitting QE at zero field is 6 x 10^{-5}, well within our experimental measurements. The fit, however, predicts a β value that is significantly less than 1, in contrast to our expectation of the field enhancement factor. Fig. 3 is a plot of the least square deviation vs.β for a laser energy of 1.98 μJ, FWHM of 14 ps and E_0 of 120 MV/m. The data deviates significantly from the prediction of the model even for β = 1. The physical origin of this low β is still under investigation.

Fig. 2a: Charge vs. RF phase, data at 120 MV/m field, 1.98 μJ laser energy.

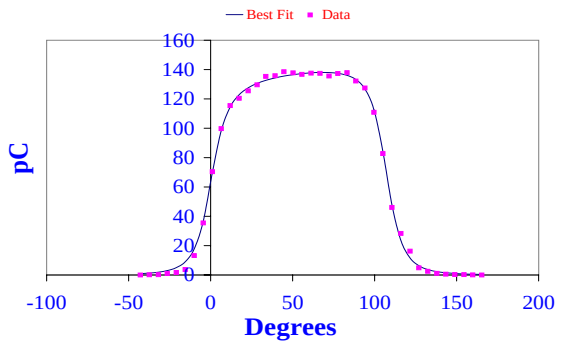

Fig. 2b: Charge vs. RF phase, data at 120 MV/m field, 10.8 μJ laser energy.

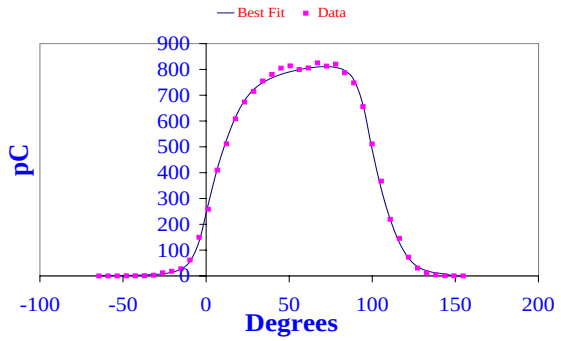

Fig. 3: Square deviation vs. β, with 120 MV/m field and 1.98 μJ laser energy.

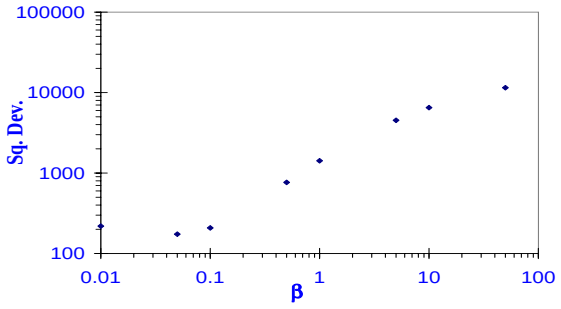

4 FUTURE PLANS

At present, Eq. 1 describes only the emission process at the cathode in the presence of the time dependent RF and space charge fields. The energy and temporal distribution of the electrons in the vicinity of the cathode in the presence of space charge, as well as the energy dependent focusing property of the solenoid are not included in the model. A more accurate model with these effects will be developed and tested against measurements. Understanding the physical origin of the low β will also be the focus of our future investigations.

5 ACKNOWLEDGMENTS

The authors would like to acknowledge the technical help of all the ATF staff and John Schill. This work was performed under the auspices of the U. S. Department of Energy under contract number DE-AC02-76CH00016.

REFERENCES

[1] C. Travier, `An introduction to Photoinjector Design', Nucl .Instr. and Meth. in Phys. Res. A340, (1994) 26-39.

[2] E. Chevallay, J. Durand, S. Hutchins, G. Suberluq, M. Wurgel,'Photocathodes Tested in the dc Gun of the CERN Photoemission Laboratory', Nucl. Instr. and Meth. in Phys. Res. A340, (1994), 146-156.

[3] P.Michelato et al. 'Charecterization of CsTe Photoemissive Film: Formation, Spectral Responses and Pollution' Proc. of FEL 1996, Aug.26-31,1996 Rome, Italy

[4] T. Srinivasan-Rao, J. Fischer, T. Tsang, 'Photoemission Studies on Metals Using Picosecond Ultraviolet Laser pulses" J. Appl. Phys (1991), 3291-3296.

[5] D. T. Palmer et al. "Commisioning Results of the Next Generation Photoinjector' presented at the 7th Advanced Accelerator Concepts Workshop, Lake Tahoe, CA Oct 13-18, 1996

[6] M. Cardona and L. Ley, in Photoemission in Solids I, edited by M. Cardona and L. Ley (Springer-Verlag, NY, 1978), p 23.

[7] M. Cardona and L. Ley, in Photoemission in Solids I, edited by M. Cardona and L. Ley (Springer-Verlag, NY, 1978), p 22.